ELSEVIER

PII: S1359-835X(97)00003-1

Composites Part A 28A (1997) 549–557

1359-835x/97/$17.00

An analysis of the fragmentation test based on aluminium matrix silicon carbide single fibre composites experiments

L. Pambaguian and R. Mevrel*
ONERA, Direction des Matériaux, 29 avenue de la Division Leclerc, B.P. 72, 92322 Châtillon Cedex, France
(Received 8 August 7995; revised 72 November 7996; accepted 5 December 7996)

Fragmentation tests have been conducted on elementary aluminium matrix/silicon carbide fibre composites. The results obtained are not consistent with Kelly and Tyson's load transfer theory widely used to determine the load transfer capacity in plastic matrix composites. From these results and the conducted observations, a model has been developed, trying to take into account the hardening of the matrix. The results obtained with this model are used to point out further necessary developments of the theory. © 1997 Elsevier Science Limited

(Keywords: aluminium matrix composite; silicon carbide fibre; micromechanical test)

INTRODUCTION

The fragmentation test is often considered as the first step in the mechanical characterisation of the interface in a long fibre-matrix composite system. It gives a parameter representative of the load transfer efficiency: the *load transfer capacity*, defined as the upper limit of the interfacial shear stress that can be attained in a given system. This test gives quantitative information and the observation of the sample after testing can also provide information regarding the different load transfer mechanisms. Moreover, one can derive from this test, an approximate dimension for the overstressed zone surrounding a fibre break in a highly-reinforced volume ratio composite.

THEORETICAL MODEL OF THE FRAGMENTATION APPLIED TO PLASTIC MATRIX COMPOSITES

Cox' analysed the reinforcement mechanism in elastic matrix/short fibre composites materials and concluded that the fibres are loaded via a shear stress transfer at the interface (from the matrix to the fibre).

Kelly and Tyson[2] worked on model composites (tungsten or molybdenum fibres embedded in copper matrix) loaded in the fibre direction. They noticed that for the lowest fibre volume ratio, the fibres were broken into several fragments after testing and defined the critical fibre volume ratio above which this phenomenon no longer appears. In agreement with the shear transfer analysis proposed by Cox, they proposed a load transfer theory applicable to plastic matrix composites.

In such composites, the rupture deformation of the reinforcement is much lower than that of the matrix and as the test proceeds, fibres break first. In the vicinity of fibre rupture, shear stress arises in the matrix and at the interface in order to reload the two fibre fragments which can then break at a later stage. Fibres continue to break (as long as the fragments are long enough to be shear-loaded up to their rupture strength) until a saturation stage is reached.

The hypothesis used for the mathematical treatment of the fragmentation theory can be schematically summarised as follows: a perfectly plastic matrix, its yield shear stress being τ_{ym}, an elastic fibre and both materials perfectly bonded.

When a fibre breaks, the matrix is plastically shear-loaded at the length required to reload the fibre. On this length, the interfacial force equilibrium can be expressed as:

$$\sigma_f(x) = 4\tau_{ym}\frac{x}{d_f} \quad (1)$$

where d_f is the fibre diameter and $\sigma_f(x)$ the tensile load in the fibre at the abscissa x.

The maximum length of a fragment at the end of the test is:

$$l_c = \frac{\sigma_{frupt}(l_c)d_f}{2\tau_{ym}} \quad (2)$$

where l_c is the critical fibre length and $\sigma_{frupt}(l_c)$ the corresponding fibre strain to failure.

* To whom correspondence should be addressed

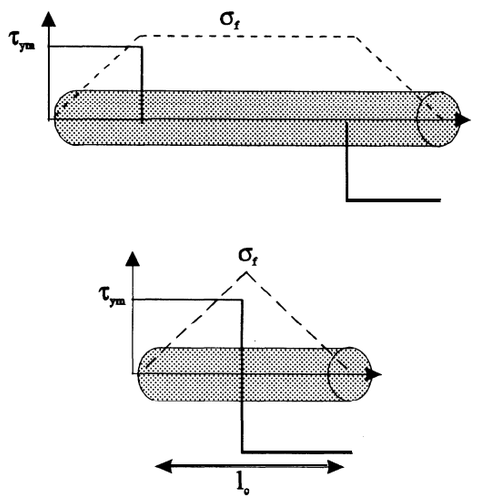

Figure 1 Variations of interfacial shear stress and load in the fibre according to Kelly and Tyson's theory: (a) during test, (b) at the saturation stage.

In this stress transfer theory, it seems important to remark that:

(1) On the fragment length where the interface is shear-loaded, the load in the fibre remains constant and the fibre can no longer break. Consequently, this length is called the ineffective length. Conversely, the length of the fibre where a rupture can occur is named the effective length.
(2) The yield shear stress of the matrix is the upper limit of the stress transfer capacity.
(3) With this model, the load in the fibre fragments cannot be expressed in terms of the macroscopic parameters characterising the traction test, i.e. the external load or strain imposed on the fragmentation sample.

Typical stress profiles in the fibre and at the interface are shown in *Figure 1*.

Fraser et *al.*[3] introduced into Kelly and Tyson's theory, the Weibull[4] statistical approach used to describe the rupture behaviour of brittle fibres (equation (3)). Using a stochastic fibre rupture model, they determined the load transfer capacity of different fibre-matrix systems.

$$Pr(\sigma) = 1 - \exp\left(-L\left(\frac{\sigma}{\beta}\right)^m\right)$$
$$\bar{\sigma} = \beta L^{-\frac{1}{m}}\Gamma\left(1+\frac{1}{m}\right) \qquad (3)$$

where L is the fibre length, m is the Weibull modulus, β is a scale parameter and $\Gamma(x)$ is the gamma function.

Finally, Ohsawa et *al.*[5] proposed a relationship between the average fragment length and the critical length (equation (4)). They presume that a fragment a little longer than l_c will break and form two fragments having length of approximately $l_c/2$. However, contrary to this, a fragment a little shorter than I, cannot break. Moreover assuming a uniform distribution of fragment lengths between the two limits, they derived for the average length the following simple expression:

$$< l > = \tfrac{3}{4} l_c \qquad (4)$$

This stress transfer theory is useful for depicting in a simple way the physical principle of reinforcement. In fact, the stress transfer process is much more complex and depends on several other effects: interfacial reaction product formation at high temperature[6] and subsequent alteration of the fibre surface[7], plastification of the matrix around reinforcement due to thermally induced stress during composite cooling[8], modification of the matrix hardening precipitation in this plastic zone during heat treatment" or stress relaxation mechanisms during testing"[9,10].

Table 1 Young's modulus (E) and yield stress ($R_{0.2}$) of the aluminium alloy matrices

Matrix	E (GPa)	$R_{0.2}$ (MPa)
Al-Cu	70	192
Al-Mg	67	81

EXPERIMENTAL AND RESULTS

Composite systems

Elementary composites constituted from an aluminium alloy matrix and a single SiC fibre have been fabricated by a liquid phase route described in detail in Ref.[12].

Matrices. Two aluminium alloys have been selected: one containing 4.5wt% copper (named Al-Cu) and a second containing 4.5wt% magnesium (named Al-Mg). These hypoeutectic alloys have been chosen so as to avoid the presence of coarse and brittle second phases which are prone to bridge fibres in high volume fraction composites, thereby being detrimental to rupture strength as they facilitate crack propagation. Only the Al-Cu alloy has been heat treated (solution treating for 24 h at 530°C, cold water quenching and natural aging 4 days). The mechanical characteristics of the matrices, determined for samples processed in the same way as the elementary composites, are listed in *Table 1*.

Fibres. Two TEXTRON fibres (SCSO and SCS2) manufactured by chemical vapour deposition (CVD), have been considered in this study. Their structure is complex and comprises:

(1) a carbon core (33 μm diameter) coated, to smooth its surface, with a one micron thick layer of pyrolytic carbon.
(2) a shell of silicon carbide deposited by CVD (thickness: 52.5 μm)
(3) in the case of SCS2, a one micron thick external deposit especially designed for incorporation onto an aluminium alloy matrix; it is mainly constituted of pyrolytic carbon and silicon carbide grains[13].

Table 2 Average strength (MPa) and Weibull modulus (m) of the fibres coated with a 2 μm aluminium layer

Fibres	$< \sigma_r >$	m
SCS0	940	4
SCS2	4540	26

. It has been demonstrated that the presence of fibre-matrix reaction product can deeply affect the fibre resistance incorporated into a composite[14]. In order to evaluate the fibre resistance inside the composite, fibres have been coated with a thin (about 2 micron thick) layer of aluminium by dipping them for 4 min in a liquid aluminium bath held at 700°C before testing. The time and temperature ranges are typical of those met in the infiltration process used to fabricate model composites. The mechanical properties of the fibres measured with a 50 mm gauge length and expressed in terms of the Weibull statistical approach are given in *Table 2*. *Figure 2* shows the corresponding Weibull plots.

Single fibre composites tests

Dog-bone test specimens (gauge length 40 mm, square section 3.5 **X** 3.5 mm^2) containing a single fibre have been used. Fragmentation tests have been conducted on a classical screw type machine with a deformation rate of $10^{-4}s^{-1}$. Three ways have been considered to gain information from tensile tests:

(1) acoustic emission signals,
(2) load drops on the force-deformation curve,
(3) visual observation of the fragments after partial dissolution of the matrix.The tests are stopped at 7.5% sample deformation, beyond which, necking can occur and the information recorded becomes too complex to be treated.

Observations and results

The acoustic emission events recorded during tensile tests present quasicontinuous spectra, both in amplitude and in duration. It is therefore not possible to assign specific phenomena to these signals *(Figure 3)*. Neither has it been possible to derive the number of fibre ruptures from the load drops on the force-deformation curve as they become too weak at the end of test and thus difficult to take into account.

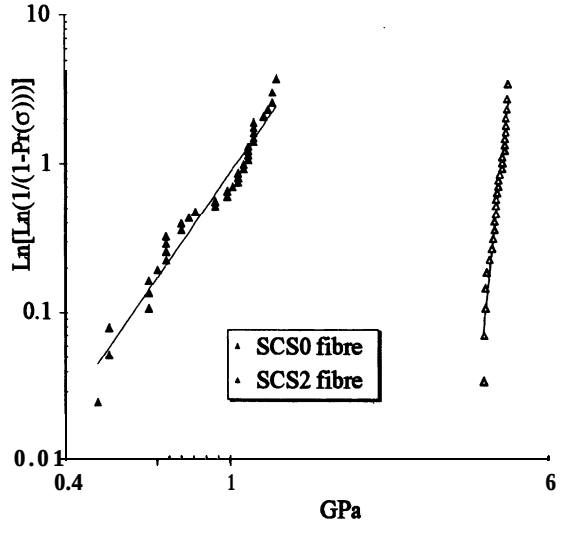

Figure 2 Weibull plots for tensile strength (50 mm gauge length) of single fibres having reacted with liquid aluminium (see text for details).

Therefore, the only way to draw information from tensile tests has been through direct observation of the fibre fragments after partial removal of the metallic matrix:

(1) In the Al–Cu/SCS0 composite system, the fibre presents longitudinal cracks and transverse ruptures. To sum up from a detailed explanation which can be found in Ref.[12], it can be said that, due to edge effects, longitudinal cracks form during the composite elaboration route *(Figure 4a)*, the tensile force applied to the specimen during testing induces their propagation *(Figure 4b)*. *No* load transfer capacity could be determined for this composite system.
(2) This phenomenon does not occur in other composite systems, for which metallographic observations on material located within the testpiece heads show that neither the fibre nor the external coating of the SCS2 fibre is broken, indicating that no fibre degradation occurs during specimen preparation.
(3) An interfacial decohesion occurs in the composites containing a SCS2 fibre. The weakest mechanical link is located at the interface between the silicon carbide and the external layer of the fibre. After testing, this layer remains bonded to the matrix and presents multiple cracking, easily observable in the gaps separating the fibre fragments. However, no such interfacial phenomenon could be detected in the Al-Mg matrix systems.

It remains difficult to determine the exact number of fibre fragments because the elastic energy released when a fragment breaks may provoke secondary (or satellite) ruptures of the fibre. On average, the number of satellite ruptures is of the same order of magnitude as the number of main ones. Nevertheless, it seems possible to separate both kinds of fibre ruptures from observation of the gap widths separating adjacent fragments. If this gap is significantly large (about one fibre diameter), one can reasonably assume that the fibre rupture is due to traction loading. On the contrary, a thin crack between two fibre fragments indicates a satellite rupture. Discarding this last type of rupture, the fragments have been counted and their length measured under an optical binocular.

From the results reported in *Figure 5* and relative to

Table 3 Fragment average length, critical length corresponding to the fibre rupture and load transfer capacity in the Al-Cu and Al-Mg matrix composites

Sample	$< l >$ (mm) [1]	$\sigma_r(l_c)$ (MPa) [2]	τ (MPa) [3]
Al-Cu SCS2 sl	1.04	5210	265
Al-Cu SCS2 s2	1.09	5200	250
Al-Mg SCS2 sl	1.23	5175	220
Al-Mg SCS2 s2	1.5	5135	180
Al-Mg SCSO sl	0.615	2630	225
Al-Mg SCSO s2	0.625	2620	220

[1] Determined from measurements of fragment lengths.
[2] Calculated from equations (3) and (4).
[3] Deduced from equation (2).

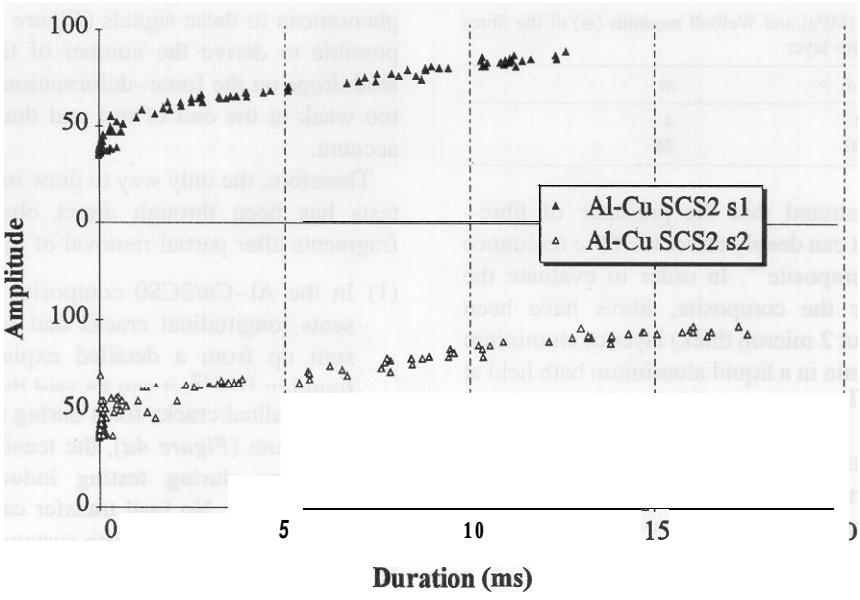

Figure 3 Amplitude versus duration plots of acoustic signals recorded during two Al–Cu matrix/SCS0 single fibre composites testing

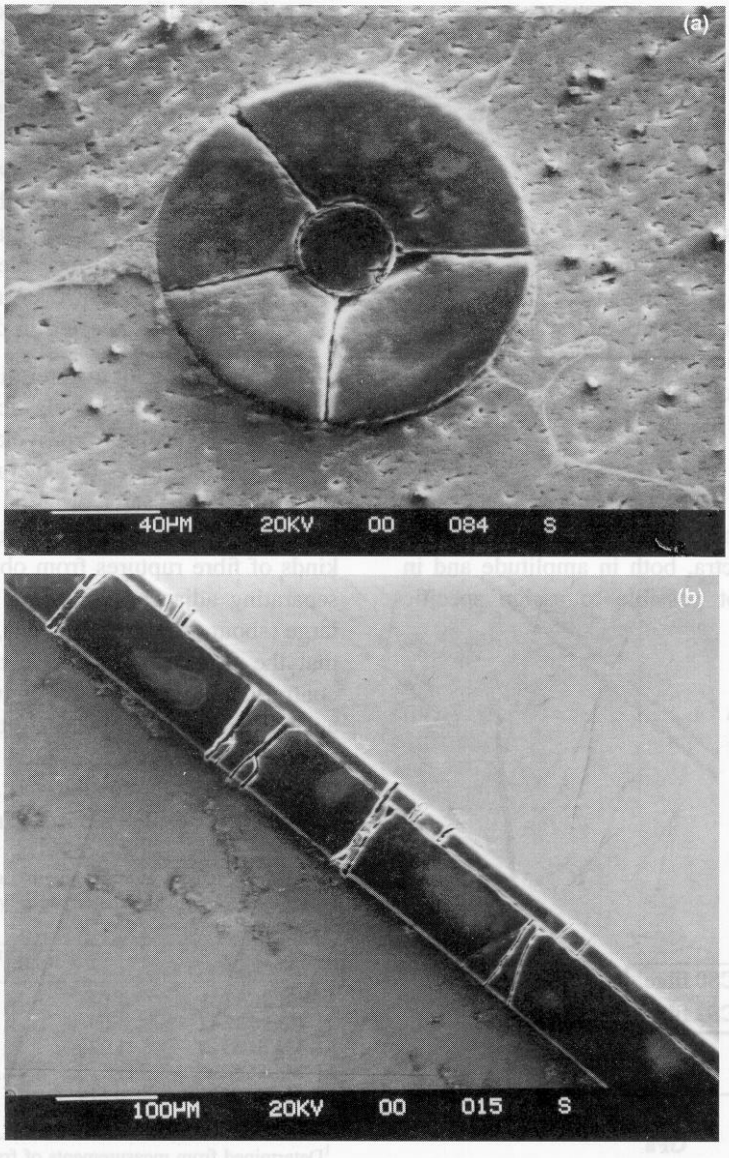

Figure 4 (a) Edge aspect of the SCS0 fibre in the Al–Cu matrix, before testing; (b) longitudinal aspect of the SCS0 fibre after testing and partial removal of the Al–Cu matrix

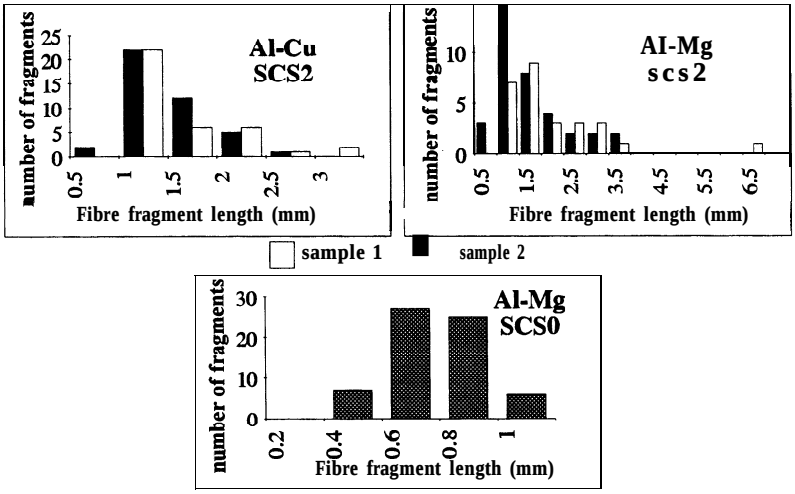

Figure 5 Distribution of fragment length measured in single fibre composite samples

fragment length measurements on two samples for each composite system, it is clear that, for a given composite system, the fragment length distribution can be significantly different from one sample to another. The load transfer capacities calculated from these distributions are reported in *Table* 3. These results pose several problems:

(1) The experimental values for τ are much higher (about 2 to 4 times) than the shear yield stress of the matrix alloy (given by $R_{0.2}/2$, see *Table 1)* which constitutes in principle the upper limit predicted by the theory.
(2) The calculated load transfer capacity can fluctuate by about 20%, from one sample test to another, for a given fibre/matrix system (e.g. Al–Mg/SCS2),
(3) The load transfer capacity can have the same value for two systems presenting very different fibre resistances and interfacial behaviours such as Al–Mg/SCS2 and Al–Mg/SCS0.

To understand the discrepancy between experimental results and predicted values, a simple fragmentation model has been developed which concentrates on examining the influence of the shear stress transfer efficiency and the fibre rupture strength on the average fragment length after test.

FRAGMENTATION TEST MODEL

The model proposed is based on Kelly and Tyson's approach. As, within that theory, it is not possible to link load supported by the fibre and external stress applied to the specimen, the model is necessarily simple and the main task consists in describing the sequence of rupture events in the fibre, the matrix acting merely as a medium capable of reloading the fibre fragments.

Background and position of the problem

Among the different fragmentation models already published[3,10,11,15,16], the one developed by Fraser[3] appears to be the most physically consistent as it presupposes no assumption on the fibre defect population. The location of the weakest point and the corresponding resistance are randomly generated according to a Weibull's distribution. It is important to remark that most other fragmentation models involve, as a first step, a partition of the simulated fibre into segments of given length and then the generation of a rupture strength value for each segment using a Weibull statistical distribution[10,11,15,16]. As a result, the simulated fibre is an 'ideal average fibre' containing all the defects described by the rupture strength distribution.

The model we propose is derived from Ref.[3] but takes into account the hardening of the matrix observed during the tensile test. On the ineffective length, the matrix is hardened and the shear stress can then be higher than the value of the matrix shear yield stress. This hypothesis can be simply expressed by replacing the term τ_{ym} of equation (1) by τ_{mat}.

At the beginning of the simulation test, a fibre of length L_i is considered, the location of its weakest point is generated at random from the Weibull distribution, as well as its rupture strength (σ_{r1}). When the load in the fibre reaches $\sigma_{r1}(\sigma_{rupt}[1] = \sigma_{r1})$, the fibre breaks into two fragments of lengths 'L_1' and 'L_2'. Then, using $\sigma_{rupt}[1]$, the ineffective length 'L_r' is derived from equation (2) according to:

$$L_r(\sigma_{rupt}[1]) = \sigma_{rupt}[1]\frac{d_f}{2\tau_{mat}}, \quad (5)$$

For both fragments thus created, the location of the weakest point and the corresponding rupture strength, according to Weibull statistics, are generated on the effective length (respectively $L_1 - L_r(\sigma_{rupt}[1])$ and $L_2 - L_r(\sigma_{rupt}[1])$).

In a subsequent step, the fragment having the lowest resistance ($\sigma_{rupt}[2]$) is determined. When the load $\sigma_{rupt}[2]$ is reached, the weakest fragment breaks into two new fragments and $\sigma_{rupt}[2]$ is used to calculate the new ineffective length. This process continues until all the fragments are shorter than the ineffective length.

It is to be noted that as this simulated test proceeds, the

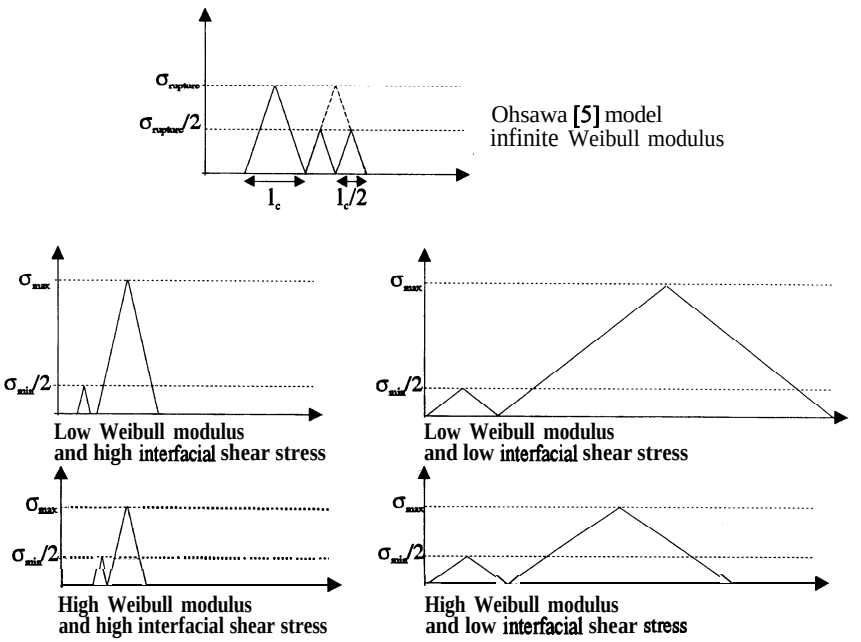

Figure 6 Geometrical construction of the fragments length limits

fibre rupture strength increases. When a fragment breaks under a load $\sigma_{rupt}[i]$, the rupture probability of the two new fragments must be zero for loads less than $\sigma_{rupt}[i]$. As the rupture strength distribution must be normalised, each fibre rupture strength is used as a proof test for the following ones. As in Fraser's model the truncated rupture strength distribution ($Pr_t(\sigma)$) is calculated from the initial distribution and expressed as:

$$Pr_t(\sigma) = \frac{Pr(\sigma) - P(\sigma = \sigma_{rupt}[i])}{1 - P(\sigma = \sigma_{rupt}[i])} \text{ when } \sigma \geq \sigma_{rupt}[i]$$
$$Pr_t(\sigma) = 0 \text{ when } \sigma < \sigma_{rupt}[i] \quad (6)$$

As rupture location and strength are associated with a fragment as soon as it is created, it may be necessary to make a second proof test. Indeed, the weakest point of a fragment can be located on the ineffective length before it provokes the rupture of the fragment. In such a case, a second weakest point is generated on the remaining effective fragment length, the weakest fragment point resistance being used in the proof test.

This algorithm satisfies other conditions neglected in previous models[10,11,15,16]. Indeed, as the saturation stage is approached, the ratio of the ineffective fibre length over the effective length increases and, as the average fibre strength depends on its total length, calculating the fibre resistance by summing up the fragment lengths leads in fact to subsequent underestimation of the resistance of the fragments. This effect could be neglected by Kelly and Tyson because the Weibull modulus of the fibres they considered was very high (about 100) and in this case, the fibre rupture strength can be considered as independent of its length. The length dependence of fibre strength also has an influence on the fragment length dispersion at the saturation stage. One can see from Figure 6 that the critical length definition proposed by Osahwa[5] is based on a geometrical construction which assumes a unique value for the fibre strength. This leads to a 2: 1 ratio between upper and lower limits for the fibre fragments at the saturation stage. In fact the fibre strength obeys Weibull statistics and a fragment can break at rather low stress values. As a consequence, the distribution of the fragment lengths at saturation is more widespread than the one considered by Osahwa, explaining why the experimental ratios reported in the literature[3,5,10,11,15,16] are actually always larger than 2.

Table 4 Mechanical characteristics of the different fibres considered in the simulation

ml $<\sigma_f>$	1 GPa	2 GPa	4 GPa
4	scso	scso [1]	
25			scs2

'Data measured on fibres dipped during 10 min in aluminium held at 700°C, and subsequent aluminium dissolution[17].

Modelling

In the simulation, the tested fibres have a gauge length of 50 mm long and their mechanical characteristics are reported in *Table* 4. Three values for $<\sigma_f>$ (1, 2 and 4 GPa) and two values for m (4 and 25) are considered, so that, among the six corresponding systems, three are representative of real fibres:

(1) SCSO: m = 4 and $<\sigma_f>$ = 1 GPa
(2) SCSO after interaction with liquid aluminum at 700°C[17]: m = 4 and $<\sigma_f>$ = 2 GPa,
(3) SCS2: m = 25 and $<\sigma_f>$ = 4 GPa.

The values selected for the interfacial shear stress (τ_{mat}) range between 50 and 200 MPa. The lower limit corresponds to the yield shear stress of the Al-Mg alloy and the upper one is about half the tensile stress of the Al-Cu matrix alloy at the end of the fragmentation test.

For each set of parameters ($<\sigma_f>, \tau_{mat}, m$), fifteen

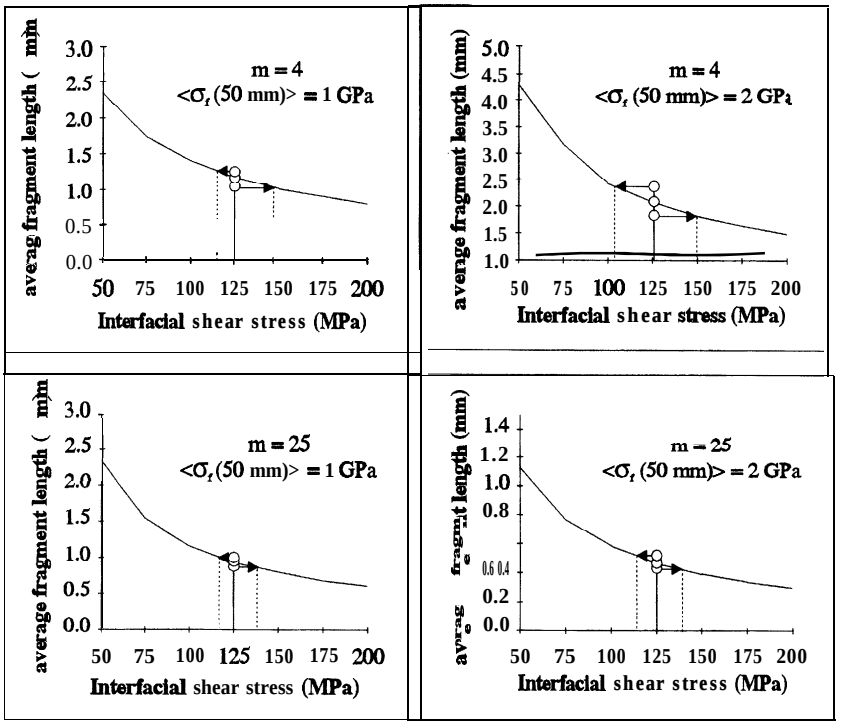

Figure 9 Average fragment length range determined from one simulated test (exact τ_{mat} = 125 MPa) and derived τ_{mat} range

The observation of the simulated average fragment length dispersion may be useful in the exploitation of real fragmentation tests. Indeed, the simulation shows that the critical fragment length can be significantly different from one test to another, and therefore a unique test could only give a rough estimate of the stress transfer capacity. Moreover, the difficulty of counting the exact number of fragments at the end of a test must not be underestimated and is susceptible to introdution of a bias in the stress transfer estimate.

In another way, the accuracy of the stress transfer capacity determination depends on the derivative of the critical length versus the stress transfer efficiency ($dl_c/d\tau_{mat}$). It can be seen on Figure 8 that this parameter decreases as the stress transfer efficiency increases. The simulated results also provide information regarding the limits of the stress transfer capacity that a single test can give. Knowing the critical fibre length limits, one can deduce the corresponding shear stress limits. Figure 9 presents examples of the interfacial shear stresses derived from average fragment length calculations. The continuous curve corresponds to simulation derived results and shows the evolution of the average fragment length $<l>$, calculated from 15 simulated tests, as a function of τ, for τ_{mat} = 125 MPa. In each graph, the maximum and minimum values for $<l>$ have also been reported. The dispersion of τ can therefore be derived from the dispersion range of $<l>$. This has important consequences for the exploitation of multifragmentation tests. For example, in the case with m = 4 and $<\sigma_f>$ = 2 GPa, a multifragmentation simulated test can lead to a τ value ranging between 105 and 150 MPa. This result explains why largely different values of τ can be obtained. Not too surprisingly, this interval is less important when m is high and/or $<\sigma_f>$ is low.

CONCLUSION

Fragmentation tests conducted on elementary aluminium matrix/silicon carbide fibre composites lead to results which are not consistent with Kelly and Tyson's load transfer theory. To explain this discrepancy, a simulation has been developed, which takes into account the matrix hardening.

This simulation of the fragmentation test permits estimation of the uncertainty relative to the critical fibre length values deduced from experimental tests. It presupposes that the fibre resistance/fibre length dependence is perfectly known as well as the number of fibre fragments. It also assumes that the shear stress transfer mechanism is perfectly described by Kelly and Tyson's theory.

For low Weibull modulus (m = 4, for example), the stress transfer capacity values deduced from experimentation are scattered on both sides of the exact value. Consequently, a large number of tests must be carried out in order to estimate accurately the stress transfer capacity in a given composite system. When the Weibull modulus is higher (m = 25, for example), fewer tests are needed.

In the case of high interfacial shear stress, the derivative of the critical length versus the shear transfer efficiency, $dl_c/d\tau_{mat}$, becomes very low, therefore:

(1) From an experimental point of view, it is necessary to know precisely the parameters characterising the fibre rupture strength as well as the number of fragments at the end of a test. The stress transfer capacity can be determined only if these conditions are fulfilled.

(2) From a practical point of view, the fragmentation test is a the useful tool for determining how the damage propagation could be avoided (or minimised) in a high fibre volume fraction composite. The simulation shows that

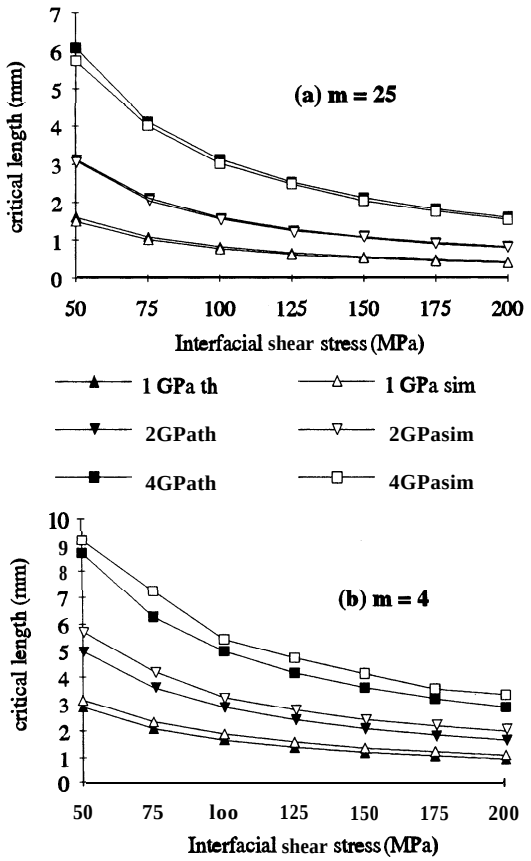

Figure 7 Critical fibre length versus interfacial shear stress; comparison between theory (dark symbols) and simulation (open symbols); (a) m = 25, (b) m = 4

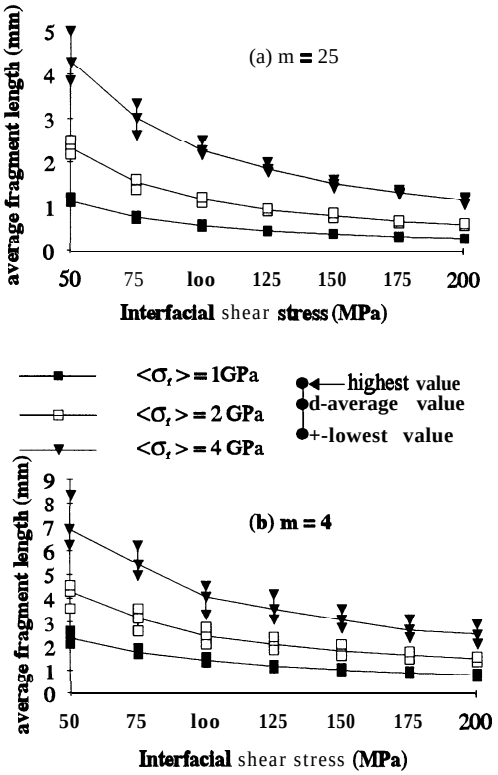

Figure 8 Average fragment lengths from simulation tests; (a) Weibull modulus: 25, (b) Weibull modulus: 4

simulation tests have been performed. This number of tests may not be sufficient for a complete statistical treatment of the results but it is largely superior to the number of fragmentation tests generally used to determine experimentally the load transfer capacity in a composite system.

Validation of the model and results

Validation. To validate this model, only the high Weibull modulus (25) has been considered in order to minimise the length dependence of fibre strength. The simulated critical length has been calculated by using equation (4) and comparing it to the theoretical value obtained by combining equations (3) and (4) (equation (7)).

$$l_c = \left[\frac{\beta\Gamma(1+\frac{1}{m})d_f}{2\tau_{mat}}\right]^{\frac{m}{(m+1)}} \qquad (7)$$

The variations of the theoretical and simulated critical fragment lengths versus the interfacial shear stress are plotted on *Figure 7a.* The discrepancy between the results given by these two calculations always remains within 7%.

As regards low Weibull modulus *(m* = 4), the same calculation shows that the shapes of the theoretical and simulated curves are similar. However, the simulated critical length is larger *(Figure 7b)* and this can be explained by two factors: (a) only the effective length is considered, to generate the fibre strength values, and (b) the proof test has a tendency to narrow the fibre strength distribution. In this case, the discrepancy between the results of both calculations can amount to about 20%.

Results. It is important to emphasise that the present algorithm generates, each time the simulation is started, a specific fibre, just as in real tests on single fibre composites. From the fifteen simulations corresponding to a single set of parameters ($<\sigma_f>, \tau_{mat}$, m), three average fragment lengths have been considered *(Figure 8):* the average calculated on all the fragments generated during the fifteen tests (taken as a reference) and the average lengths corresponding to the tests giving the lowest and the highest numbers of fragments. These last lengths give an indication of the dispersion of the critical length (which is identical to the average length).

It can be seen that the fragment length dispersion is important whatever the Weibull modulus of the fibre. This dispersion increases as the interfacial shear stress decreases or as the fibre resistance increases because the number of fragments obtained at the end of the simulation is low.

When the number of fragments is higher, that is for low fibre resistance or large interfacial shear stress, the average fragment length obtained at the end of a test can differ by about 5–7% from the reference. In this case, the influence of the number of fragments on the dispersion is less marked and it is mainly due to the coupling of a geometrical factor (the ineffective length) and a statistical criterion (the generation mode of defect location and rupture strength).

(in the case of perfect interfacial bonding), when the matrix is 'hard enough', the critical fibre length remains practically the same over a wide range of interfacial shear stress. Since the critical length (or the length necessary to reload a fibre fragment) becomes nearly independent of the inter-facial shear stress, the choice of the matrix should therefore be guided by parameters other than the load transfer capacity: for example transverse strength of the composite, corrosion resistance or temperature of matrix liquidus.

REFERENCES

1. Cox, H.L., The elasticity and strength of paper and other fibrous materials. *Brit. J. Appl. Phys., 1952, 3, 72.*
2. Kelly, A. and Tyson, W.R., Tensile properties of fibre-reinforced metals: copper/tungsten and coper/molybdenum. *J. Mech. Phys. Solids, 1965, 13, 329.*
3. Fraser, W.A., Ancker, F.H. and Di Benedetto, A.T., A computer modeled single filament technique for measuring coupling and sizing agent effects in fibre reinforced composites. In *Proceedings of the 30th Annual Technical Conference of the Reinforced Plastics/ Composites Institute,* Section 22-A. The Society of the Plastics Industry Inc., Washington, 1975, p. 1.
4. Weibull, W., A statistical distribution function of wide applicability. *J. Appl. Mech., 1951,* **18,** *293.*
5. Ohsawa, T., Nakayama, A., Miwa, M. and Hasegawa, A., Temperature dependence of the critical fibre length for the glass fibre-reinforced thermosetting resins. *J. Appl. Polym. Sci., 1978, 22, 3203.*
6. Viala, J.C., Fortier, P. and Bouix, J., Stable and metastable phase equilibria in the chemical interaction between aluminium and silicon carbide. *J. Mater. Sci., 1990, 25, 1842.*
7. Pelletier, S., Elaboration et caractérisation de composites C/Al: infiltration de mèches de fibres traitées. These de doctorat de l'Ecole Nationale Supérieure des Mines de Paris, 1994.
8. Flom, Y. and Arsenault, R.J., Deformation in Al/SiC composites due to thermal stresses. *Mater. Sci. Engng, 1985, 75, 151.*
9. Salvo, L., Comportement au durcissement structural de matériaux composites à matrice aluminium renforcee de particules c eramiques: cas des systèmes 6061/SiC et 6061/Al_2O_3. These de doctorat de l'Institut National Polytechnique de Grenoble, 1992.
10. Jacques, D., Transfert de charge entre fibre et matrice dans les composites carbone résine. Comportement en traction d'un composite modèle monofilamentaire. These de doctorat, Institut Polytechnique de Lorraine, Nancy, 1989.
11. Feillard, P., Contribution à l'étude micromecanique de l'interface et des phénomènes élémentaires d'endommagement dans les composites modèles fibre de verre/résine epoxyde, These de doctorat de l'Institut National des Sciences Appliquées de Lyon, 1993.
12. Pambaguian, L., Etude du comportement mecanique des interfaces dans des composites monofilamentaire à matrice en alliage d'aluminium renforcés par des fibres en carbure de silicium. These de doctorat de l'Université Paris-Sud, Orsay, 1994.
13. Nutt, R.S. and Wawner, F.E., Silicon carbide filaments microstructure. *J. Mater. Sci., 1985, 20, 1953.*
14. Pambaguian, L. and Mevrel, R., Fibre strength selection and the mechanical resistance of fibre-reinforced metal matrix composites. *J. Mater. Sci., 1996, 31, 5215-5220.*
15. Ochiai, S. and Osamura, K., Multiple fracture of a fibre in a single tungsten fibre-copper matrix composite. *Zeitschrift für Metallkunde Bd., 1986,* **77**(H4), *225.*
16. Lacroix, Th., Tilmans, B., Keunings, R., Desaeger, M. and Verpoest, I., Modelling of critical fibre length and interfacial debonding in the fragmentation testing of polymer composites. *Compos. Sci. Technol., 1992, 43, 379.*
17. Wawner, F.E. and Nutt, S.R., Investigation of diffusion barrier materials on silicon carbide filaments. *Ceram. Engng Sci. Proc. No. 7-8, 1989,* **1,** *709.*